Supplementary Information

The First Coordination Polymers with an $[O]_2[N]P(S)$-Hg Segment: A Combined Experimental, Theoretical and Database Study

Elham Torabi Farkhani[a], Mehrdad Pourayoubi[a,]*, Mohammad Izadyar[a], Pavel V. Andreev[b], Ekaterina S. Shchegravina[c]

[a]*Department of Chemistry, Faculty of Science, Ferdowsi University of Mashhad, Mashhad, Iran*

[b]*Department of Physics, N. I. Lobachevsky State University of Nizhni Novgorod, pr. Gagarina, 23-3, Nizhni Novgorod, Russia*

[c]*Department of Chemistry, Lobachevsky State University of Nizhni Novgorod, Gagarin Avenue, 23, Nizhni Novgorod, Russia*

*****E-mail: pourayoubi@um.ac.ir*

Contents

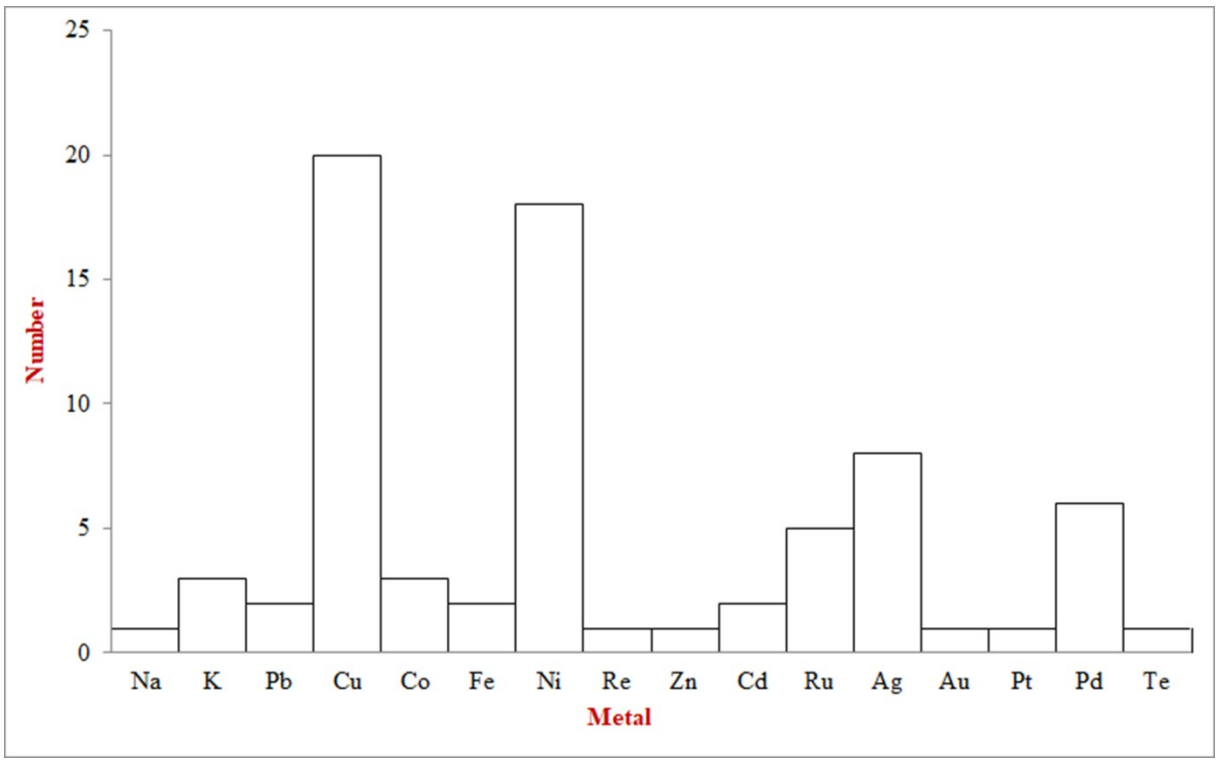

Figure S1. Histogram of the number of the reported complexes with a free ligand containing an $[O]_2P(S)[N]$ segment. Reported data were obtained from CSD.

	1	**2**	**3**
Empirical formula	$C_7H_{13}Cl_2HgNO_2PS$	$C_{14}H_{26}Br_2HgN_2O_4P_2S_2$	$C_6H_{14}Cl_2HgNO_2PS$
Formula weight	477.7	772.84	466.72
Temperature (K)	293 (2)	293 (2)	293 (2)
Wavelength (Å)	0.71073	0.71073	0.71073
Crystal system	Triclinic	Monoclinic	Orthorhombic
Space group	$P\bar{1}$	$P2_1/c$	*Pbca*
a (Å)	7.5816 (3)	18.5214 (10)	11.6229 (4)
b (Å)	7.6514 (4)	8.3511 (3)	17.2516 (4)
c (Å)	12.7568 (5)	18.379 (1)	13.2057 (4)
α (˚)	101.717 (4)	90.00	90.00
β (˚)	104.651 (4)	118.740 (7)	90.00
γ (˚)	102.378 (4)	90.00	90.00
V (Å^3)	672.89 (5)	2492.6 (3)	2647.92 (14)
Z	2	4	8
D_{calc} (g/cm^3)	2.358	2.059	2.341
Absorption coefficient (mm^{-1})	12.088	9.698	12.284
F (000)	446	1472	1744
Crystal size (mm)	0.221 × 0.101 × 0.0397	0.186 × 0.175 × 0.121	0.339 × 0.315 × 0.272
θ Range for data collection (˚)	3.77 – 32.513	4.105 – 28.502	3.506 – 26.372
Index ranges	$-9 \le h \le 9$	$-23 \le h \le 23$	$-14 \le h \le 14$
	$-9 \le k \le 9$	$-10 \le k \le 10$	$-21 \le k \le 21$
	$-15 \le l \le 15$	$-22 \le l \le 22$	$-16 \le l \le 16$
Reflections collected	11432	52536	38870
Independent reflections	2745 [R_{int} = 0.0336]	5093 [R_{int} = 0.036]	2708[R_{int} = 0.0530]
Min and max transmission	0.293 and 1.000	0.294 and 0.458	0.06 and 0.123
Refinement method	full-matrix least-squares on F^2	full-matrix least-squares on F^2	full-matrix least-squares on F^2
Data/restraints/parameters	2745/1/142	5093/1/244	2708/2/128
Goodness-of-fit on F^2	1.042	1.027	1.179
Final *R* indices [$I > 2\sigma(I)$]	R_1 = 0.0188, wR_2 = 0.0424	R_1 = 0.0286, wR_2 = 0.0648	R_1 = 0.0426, wR_2 = 0.0802
R indices (all data)	R_1 = 0.0207, wR_2 = 0.0431	R_1 = 0.0380, wR_2 = 0.0690	R_1 = 0.0541, wR_2 = 0.0835
The largest difference in peak and hole (e Å^{-3})	0.68 and –0.80	0.822 and –0.637	0.74 and –1.011

Table S1. Crystal data and structure refinement for **1**, **2** and **3**.

Table S2. Selected experimental and optimized bond distances (Å) and angles (°) for **1**, **2** and **3**.

1	Experimental	Optimized		Experimental	Optimized
Hg1—S1	2.4444 (8)	2.4445	S1—P1	1.9765 (10)	1.9864
Hg1—Cl1	2.4290 (9)	2.4294	N1—P1	1.622 (2)	1.6536
Hg1—Cl2	2.4864 (8)	2.4852	N1—H1	0.845 (18)	1.0100
Hg1—Cl2^{ii}	2.8276 (8)	2.8419	N1—C1	1.429 (4)	1.4228
Cl2—Hg1^{i}	2.8276 (8)	2.8526	Hg1—Cl2—Hg1^{i}	93.09 (2)	90.37
Cl1—Hg1—S1	125.46 (4)	119.89	P1—S1—Hg1	100.82 (4)	99.36
Cl2—Hg1—S1	118.69 (3)	114.73	O1—P1—S1	115.68 (9)	115.65
Cl2^{i}—Hg1—S1	108.49 (3)	96.08	O2—P1—S1	116.80 (10)	117.72
Cl1—Hg1—Cl2	111.08 (4)	116.87	N1—P1—S1	105.25 (9)	106.67
Cl1—Hg1—Cl2^{i}	94.56 (3)	114.21	P1—N1—H1	118 (3)	116.97
Cl2—Hg1—Cl2^{i}	86.91 (3)	87.93	C1—N1—H1	115 (3)	116.57
2					
Hg1—S1	2.6625 (13)	2.6611	P1—N1	1.621 (4)	1.6394
Hg1—S2	2.6076 (11)	2.6073	P2—N2	1.638 (3)	1.6576
Hg1—Br1	2.5338 (5)	2.5480	N1—H1	0.8600	1.0099
Hg1—Br2	2.5482 (5)	2.5344	N2—H2	0.8600	1.0095
S1—P1	1.9688 (17)	1.9731	N1—C1	1.428 (5)	1.4188
S2—P2	1.9694 (14)	1.9755	N2—C8	1.428 (5)	1.4098
Br1—Hg1—S1	104.97 (3)	105.07	O1—P1—S1	112.54 (15)	112.86
Br1—Hg1—S2	106.05 (3)	108.28	O2—P1—S1	115.70 (15)	115.39
Br2—Hg1—S1	105.12 (3)	110.58	N1—P1—S1	111.21 (15)	112.94
Br2—Hg1—S2	117.82 (3)	103.74	O3—P2—S2	115.36 (13)	115.41
S1—Hg1—S2	99.42 (4)	95.26	O4—P2—S2	115.82 (12)	116.34
Br1—Hg1—Br2	120.55 (19)	128.83	N2—P2—S2	108.02 (13)	108.46
P1—S1—Hg1	102.38 (6)	103.40	P2—S2—Hg1	96.76 (5)	98.52
3					
Hg1—S1	2.447 (2)	2.4500	S1—P1	1.986 (3)	2.0026
Hg1—Cl1	2.369 (3)	2.3686	P1—N1	1.610 (6)	1.6459
Hg1—Cl2	2.590 (2)	2.8511	P1—O1	1.545 (6)	1.5738
Hg1—Cl2^{i}	2.681 (2)	2.5901	P1—O2	1.556 (6)	1.5778
Cl2—Hg1^{i}	2.681 (2)	2.8512	Hg1—Cl2—Hg1^{i}	92.56 (7)	92.98
Cl1—Hg1—S1	130.86 (8)	127.62	P1—S1—Hg1	98.49 (10)	102.86
Cl2—Hg1—S1	104.65 (8)	105.90	O1—P1—S1	115.7 (3)	113.13
Cl2^{i}—Hg1—S1	105.96 (8)	98.76	O2—P1—S1	101.6 (2)	103.85
Cl1—Hg1—Cl2	110.97 (9)	104.68	N1—P1—S1	115.8 (2)	116.81
Cl1—Hg1—Cl2^{i}	108.33 (10)	108.86	N1—P1—O1	102.4 (3)	101.73
Cl2—Hg1—Cl2^{i}	87.44 (7)	86.51	N1—P1—O2	112.4 (3)	106.18

Symmetry codes: **1**: (i) $-x + 1, -y + 2, -z + 1$; (ii) $-x + 3, -y + 2, -z + 2$; **2**: (i) $-x + 1, -y + 1, -z + 1$; (ii) $-x, -y + 1, -z$; **3**: (i) $-x, -y + 1, -z$.

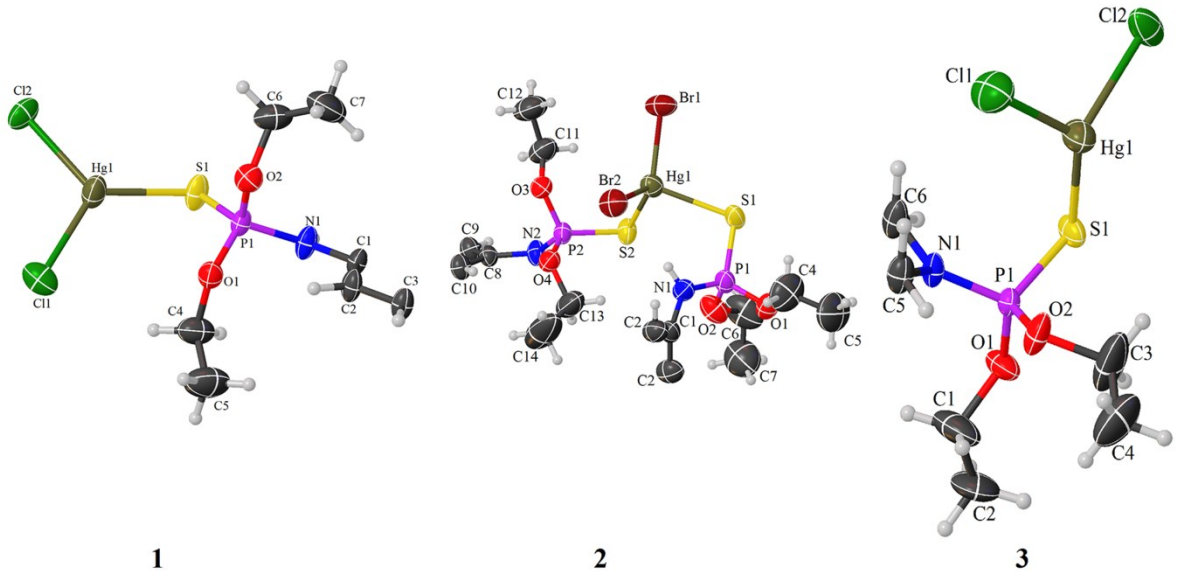

Figure S2. Displacement ellipsoid plots of the asymmetric units of **1**, **2** and **3** (50 % probability).

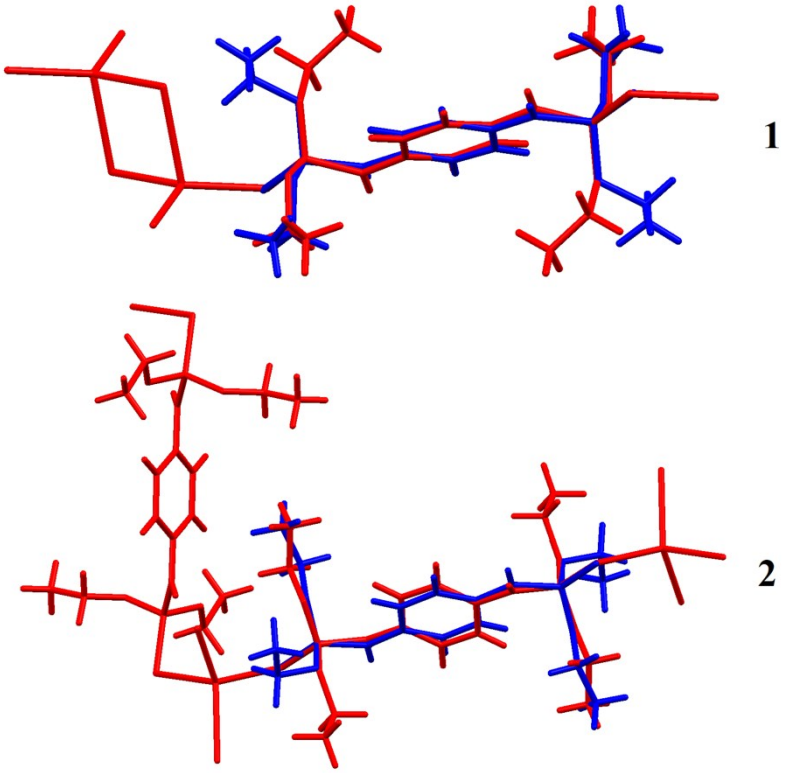

Figure S3. Best overlay for two **1**, **2** and L_1. **1**/**2** and L_1 have been represented as red and blue colors, respectively.

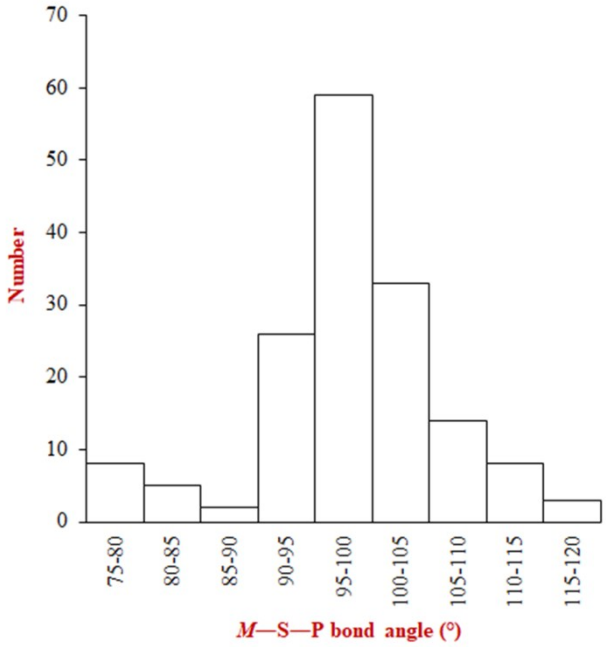

Figure S4. Histogram of the *M*—S—P bond angles for complexes with an [N]P(S)[O]$_2$-based ligands (where *M* is a metal). Reported data were obtained from CSD.

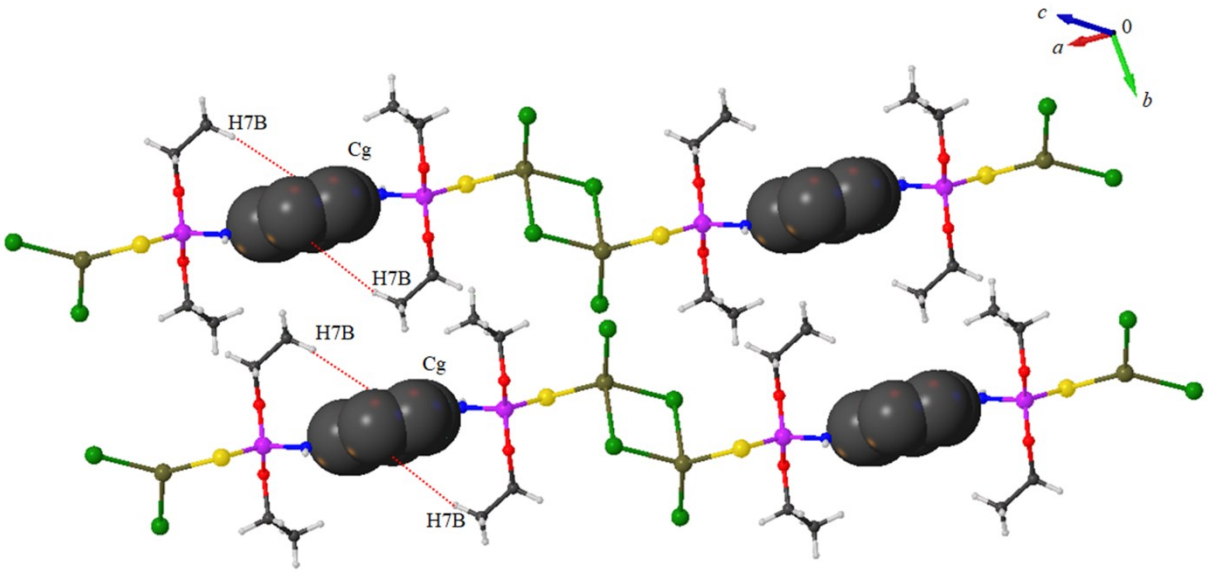

Figure S5. The C—H···π interaction in **1** (red dashed line).

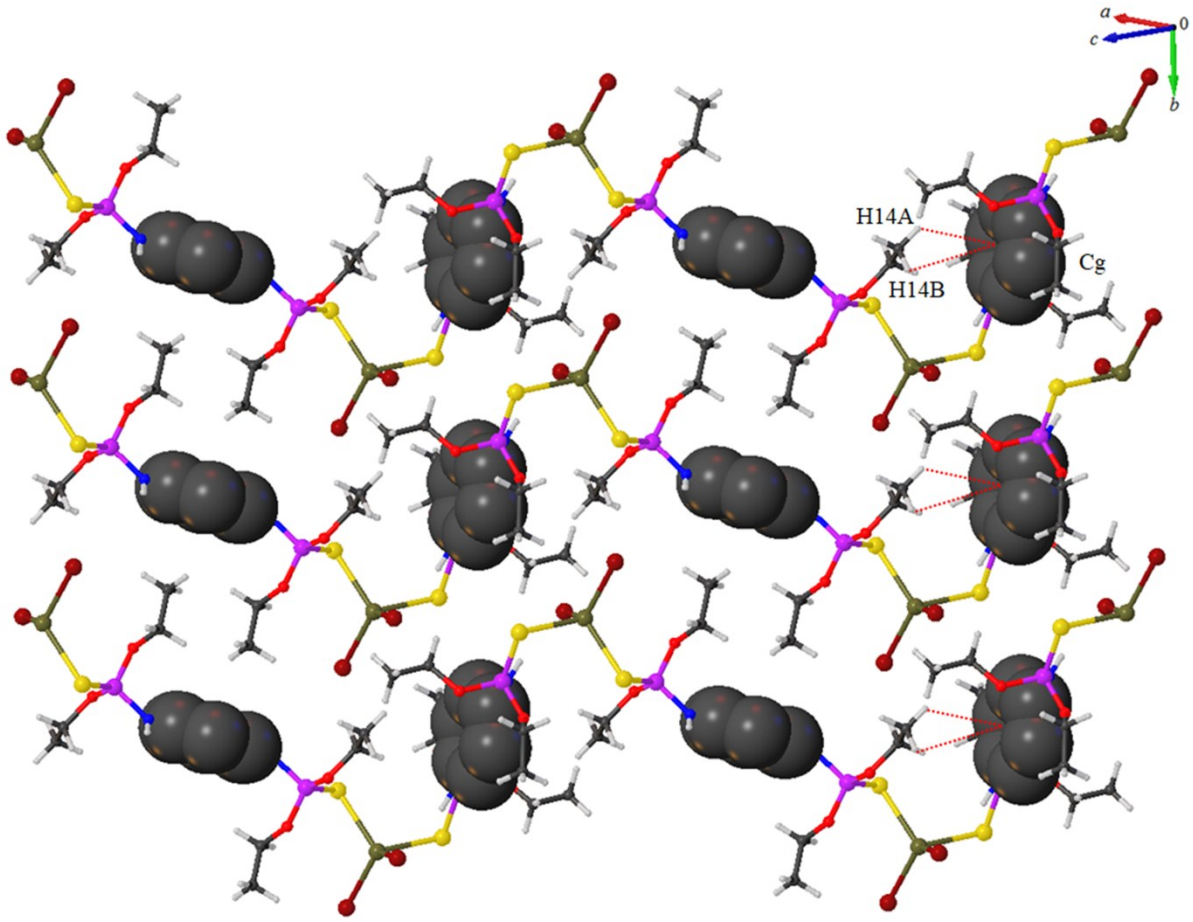

Figure S6. The C—H···π interactions in **2** (red dashed line).

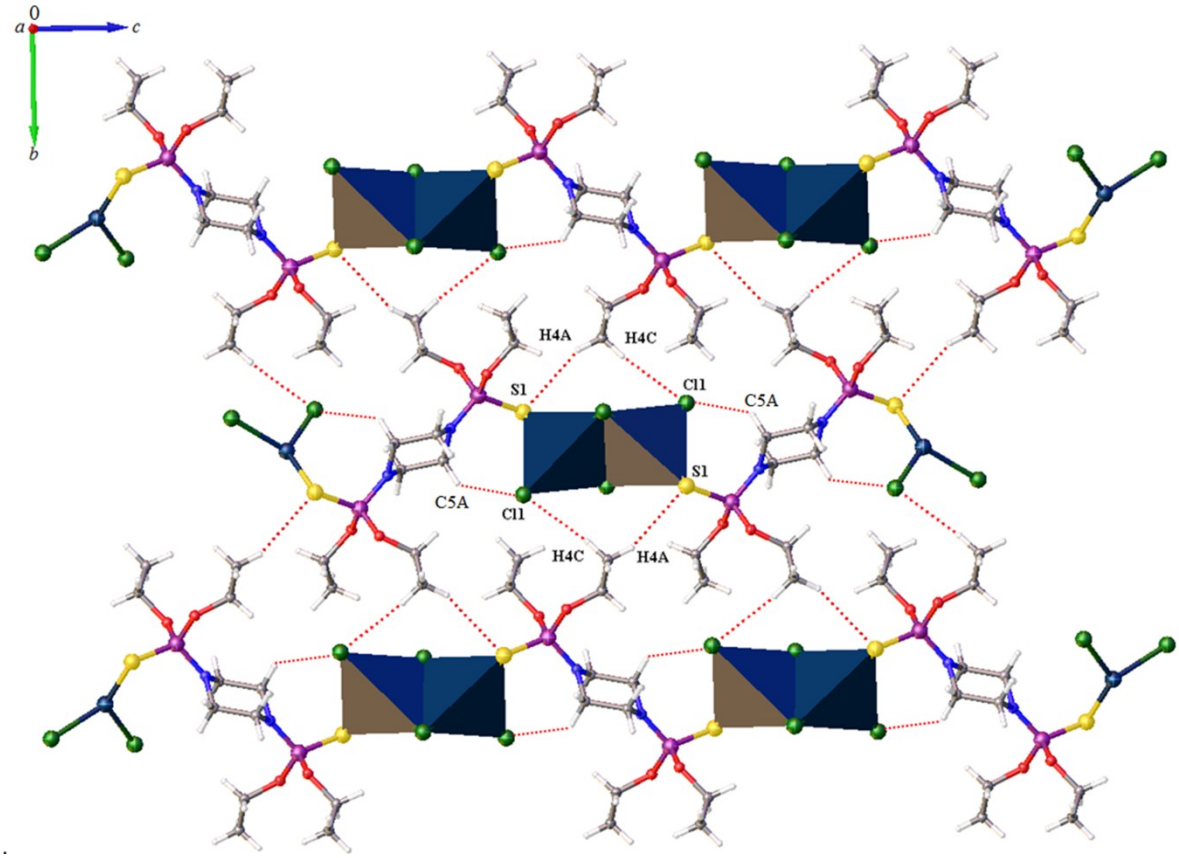

Figure S7. The two-dimensional array of **3**, built from C—H···Cl and C—H···S interactions. Polyhedra representation was used for showing the coordination sphere of mercury.

Table S3. QTAIM parameters (in a.u.) at M06-2X/6-311++G(d,p)/LANL2DZ level.

	$\rho(\mathbf{r})$	$\nabla^2\rho(\mathbf{r})$	$\lvert V(\mathbf{r})\rvert/G(\mathbf{r})$	$H(\mathbf{r})$
1				
Hg–S	0.67, 0.67	0.17, 0.16	1.30, 1.30	–0.18, –0.18
Hg–Cl terminal	0.63, 0.64	0.23, 0.22	1.18, 1.18	–0.12, –0.12
Hg–Cl bridge	0.57, 0.57	0.21, 0.20	1.15, 1.15	–0.09, –0.09
N1—H1···Cl1	0.14	0.52	0.88	0.01
C2—H2···O1	0.14	0.61	0.80	0.02
C4—H4*A*···Cl1	0.85	0.30	0.79	0.13
C7—H7*B*···Cg	0.35	0.16	0.52	0.13
2				
Hg–S	0.49, 0.45	0.15, 0.14	1.17, 1.14	–0.08, –0.06
Hg–Br	0.59, 0.57	0.62, 0.68	1.50, 1.46	–0.16, –0.14
N1—H1···Br2	0.14	0.22	1.10	0.06
C4—H4*A*···Br2	0.84	0.18	0.87	0.03
C13—H13*B*···Br1	0.96	0.19	0.92	0.05
C10—H10···Br1	0.89	0.19	0.87	0.05
C4—H4*B*···S1	0.77	0.26	0.74	0.14
C11—H11*B*···S2	0.71	0.19	0.92	0.03
C9—H9···O4	0.27	0.10	0.84	0.06
C3—H3···O2	0.11	0.50	0.74	0.26
C14—H14*A*···Cg	0.65	0.28	0.66	0.18
C14—H14*B*···Cg	0.40	0.12	0.56	0.12
3				
Hg–S	0.67, 0.67	0.16, 0.16	1.30, 1.30	–0.18, –0.18
Hg–Cl terminal	0.71, 0.71	0.25, 0.25	1.20, 1.20	–0.16, –0.16
Hg–Cl bridge	0.47, 0.47	0.17, 0.17	1.11, 1.11	–0.05, –0.05
C4—H4*C*···Cl1	0.12	0.40	0.84	0.13
C5—H5*A*···Cl1	0.10	0.35	0.83	0.13
C4—H4*A*···S1	0.85	0.28	0.73	0.15

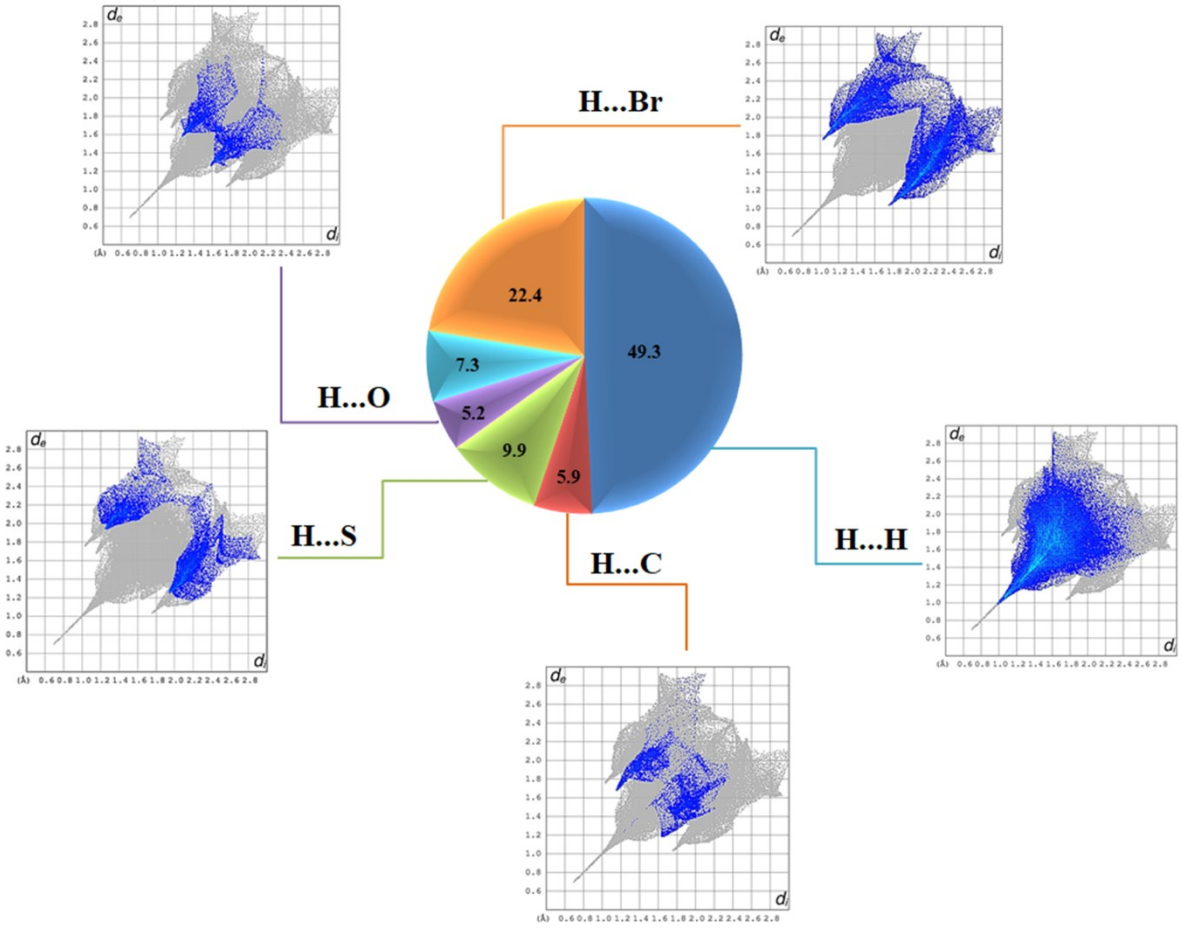

Figure S8. Schematic illustration of the fingerprint plots of **2**. Different colors have been used for different atom pair contacts.

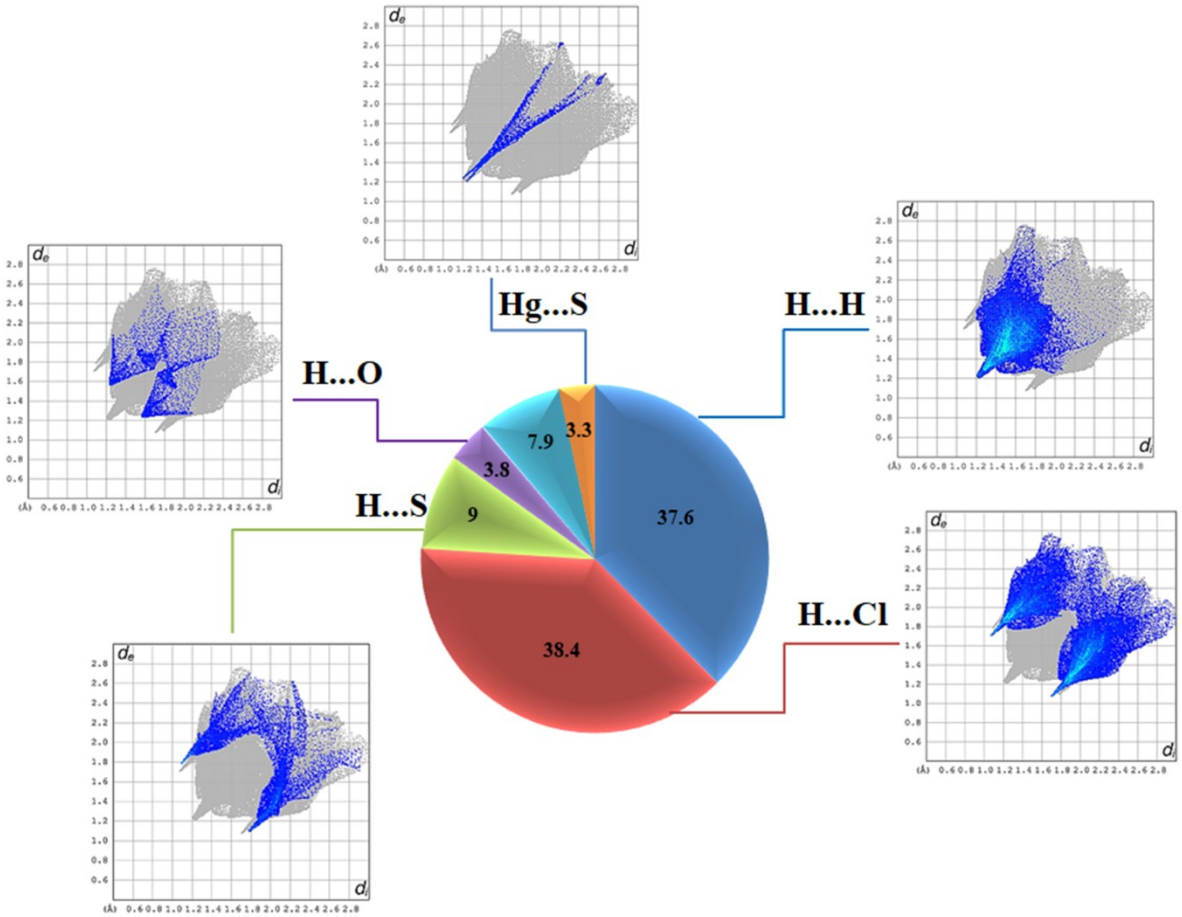

Figure S9. Schematic illustration of the fingerprint plots of **3**. Different colors have been used for different atom pair contacts.

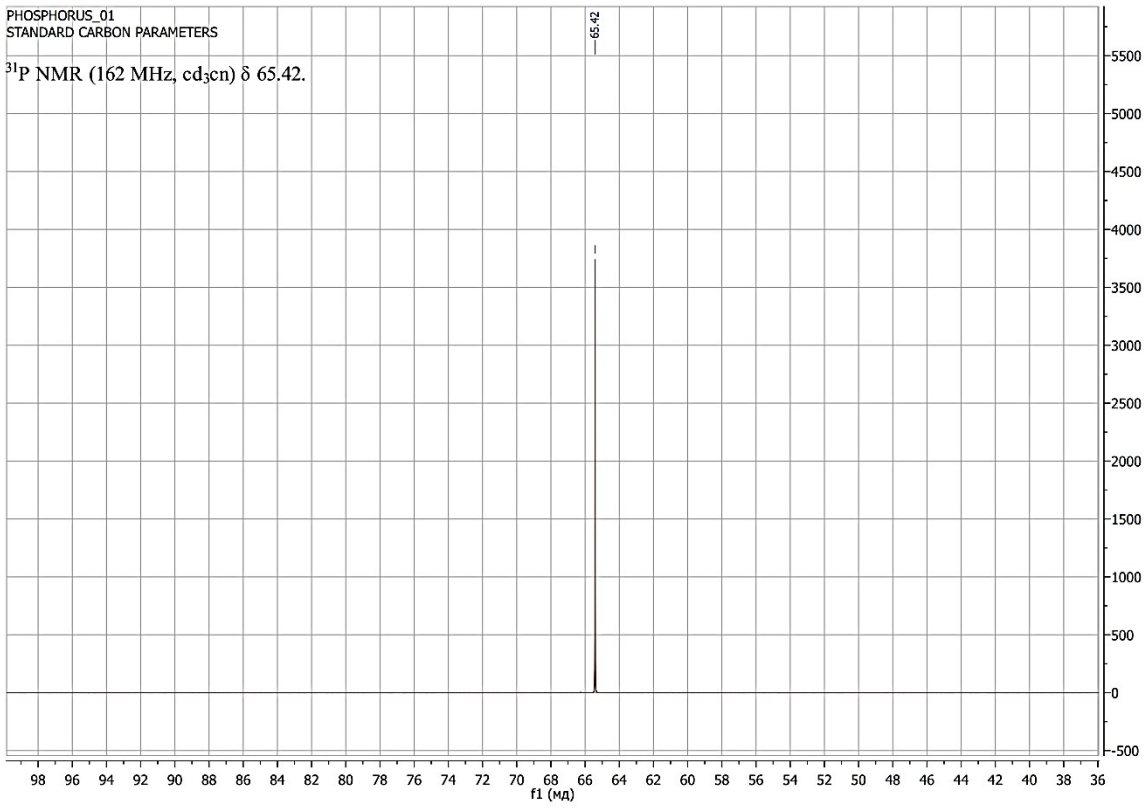

Figure S10. $^{31}P\{^{1}H\}$ NMR for L_1.

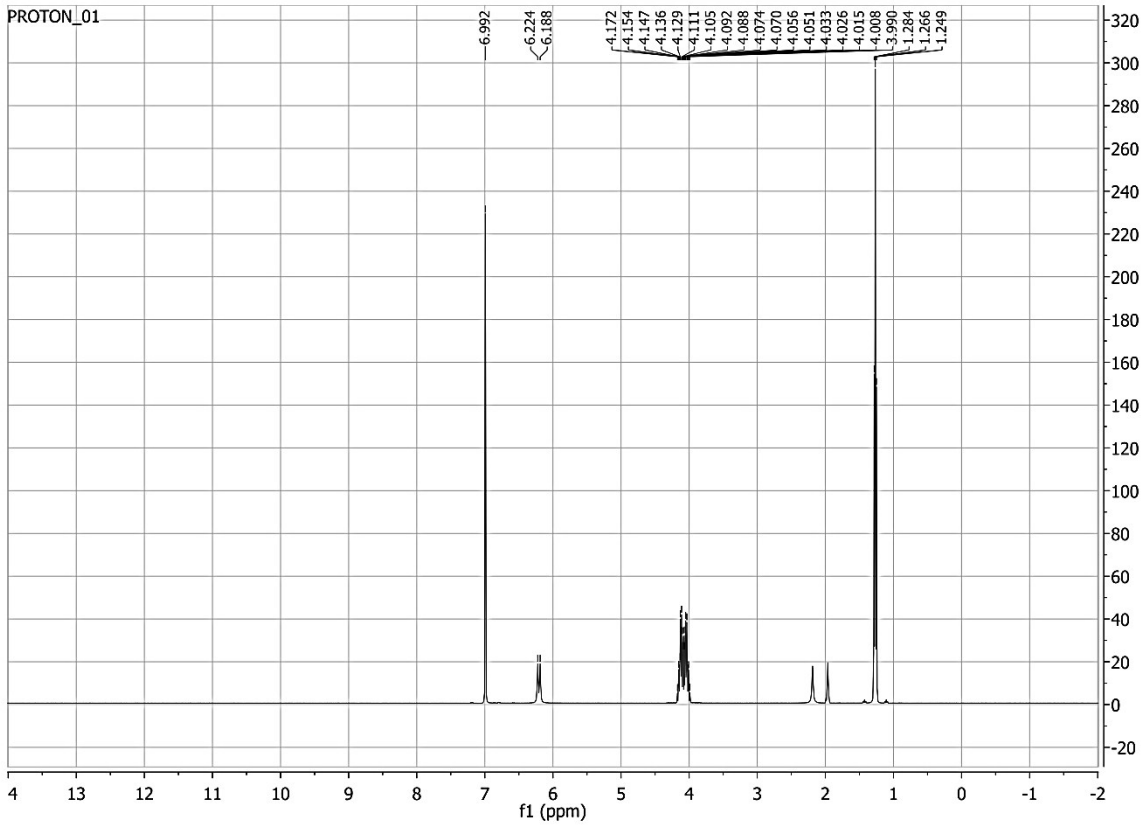

Figure S11. ^{1}H NMR for L_1.

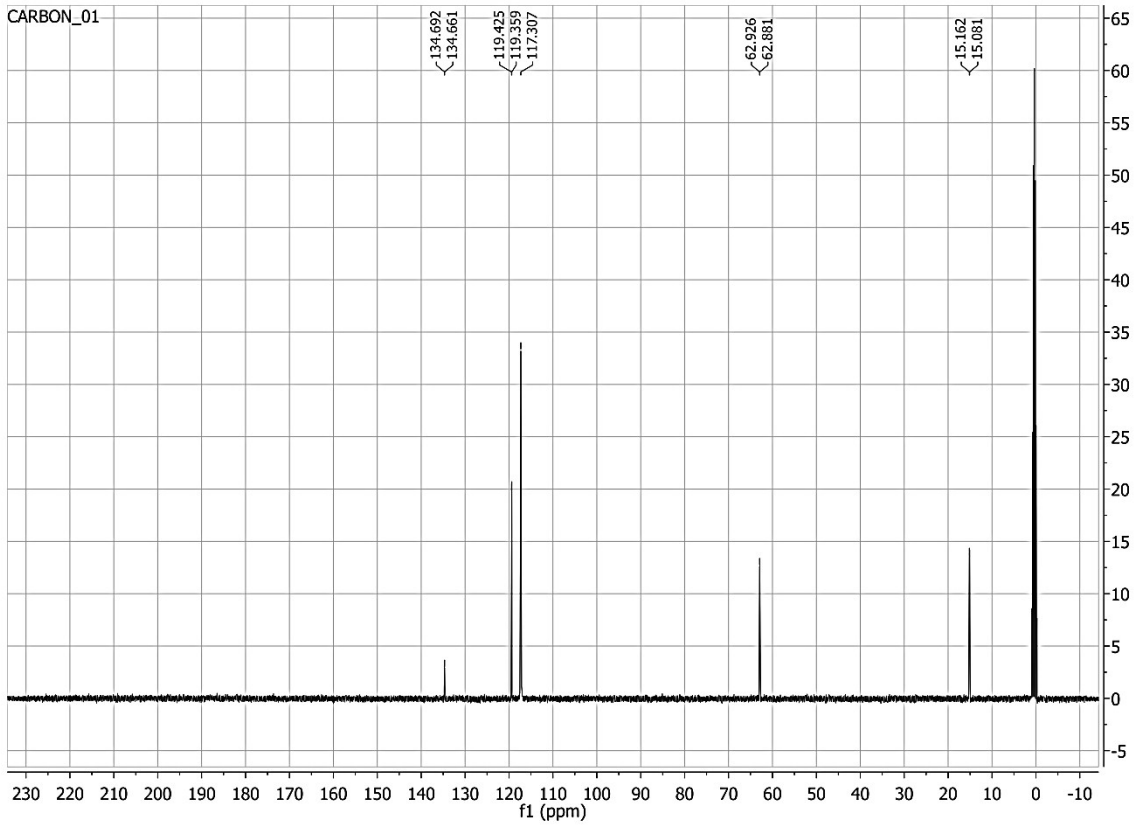

Figure S12. ^{13}C NMR for L_1.

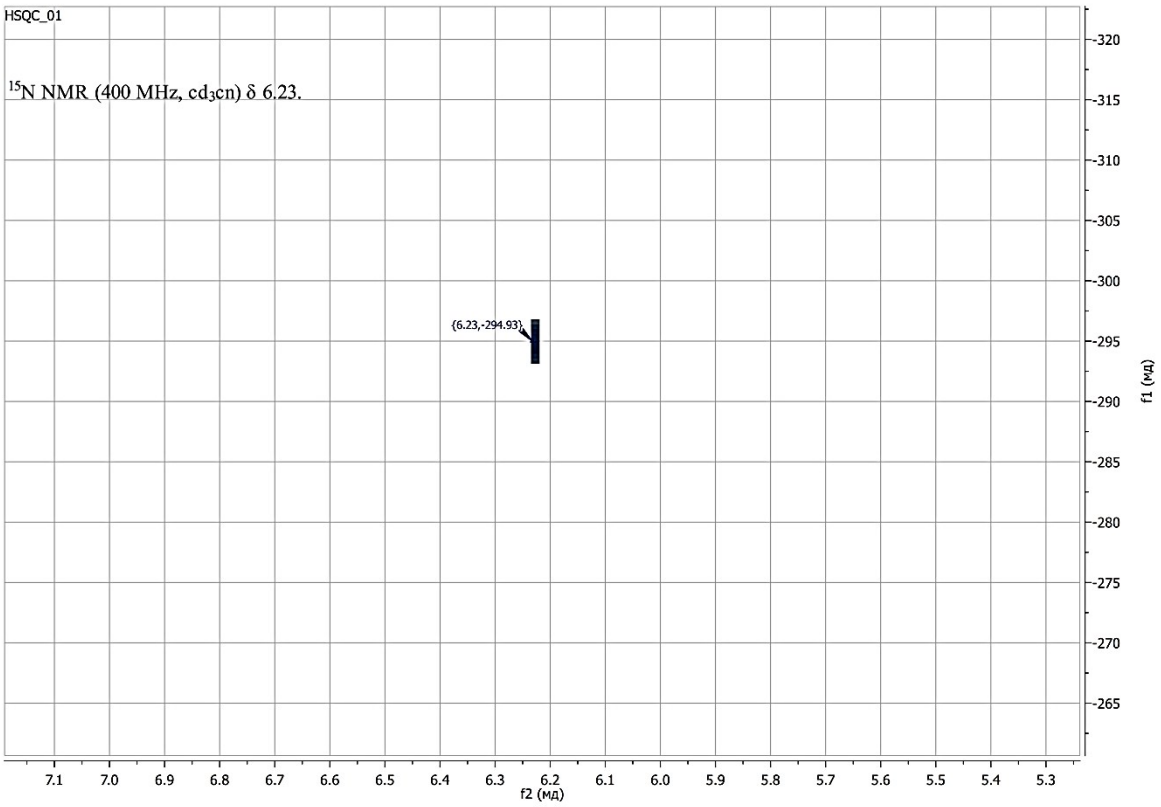

Figure S13. ^{1}H-^{15}N HSQC for L_1.

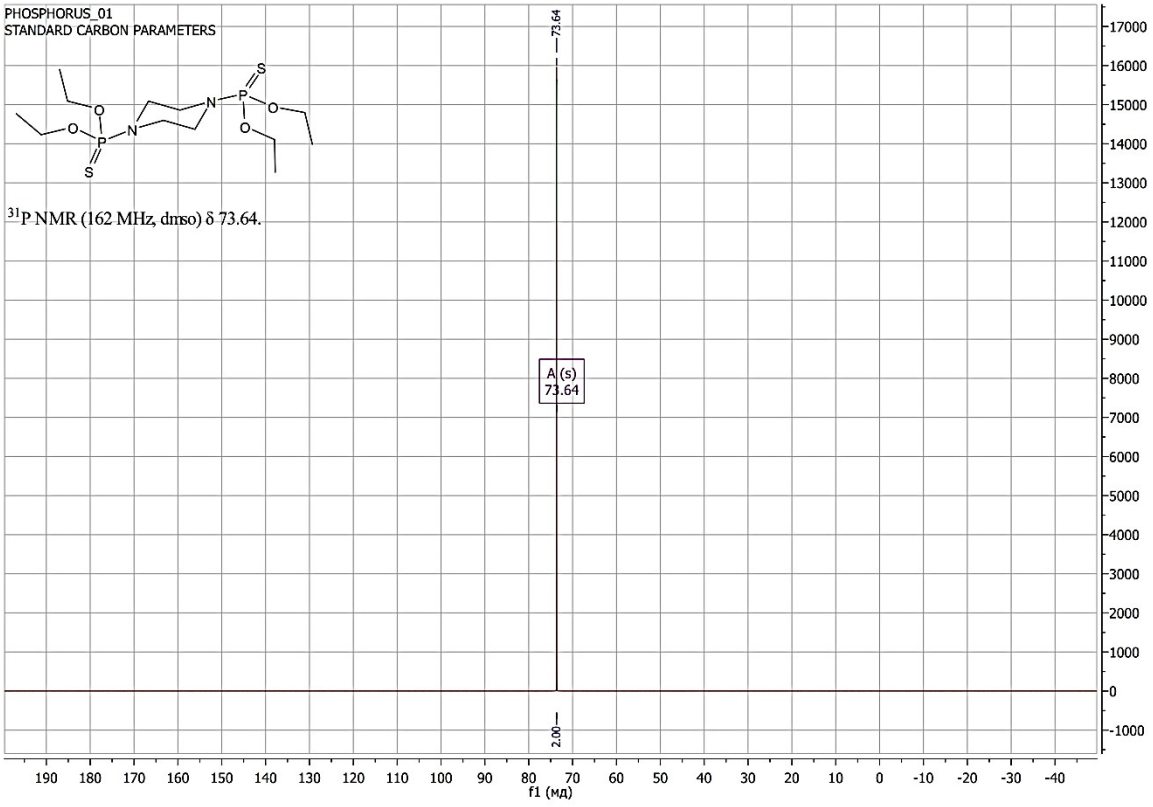

Figure S14. $^{31}P\{^{1}H\}$ NMR for L_2.

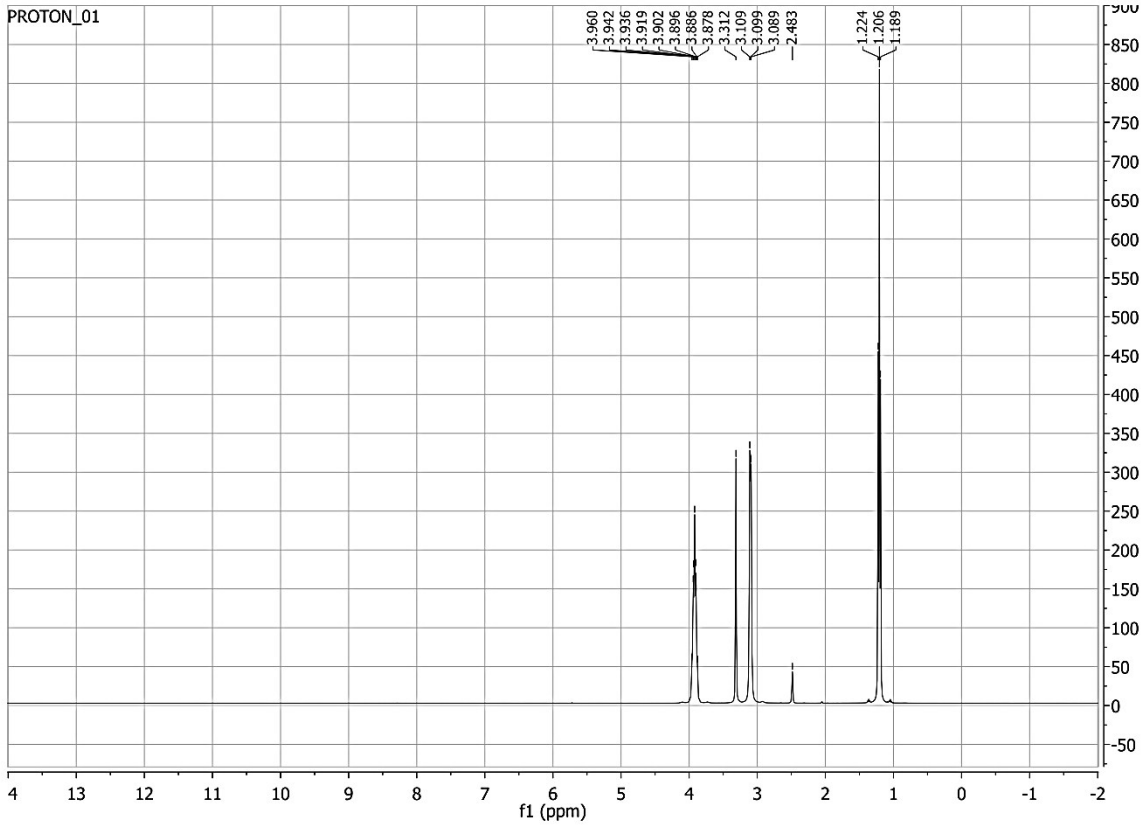

Figure S15. ^{1}H NMR for L_2.

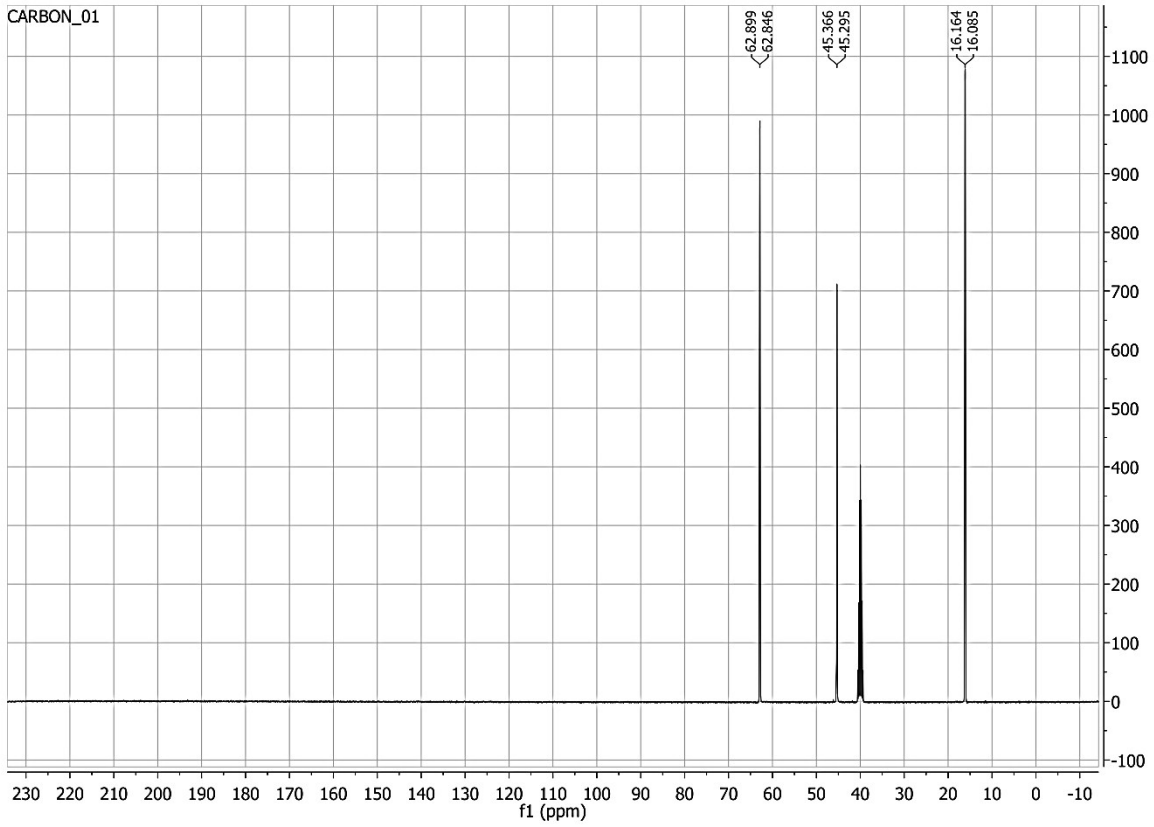

Figure S16. ^{13}C NMR for L_2.

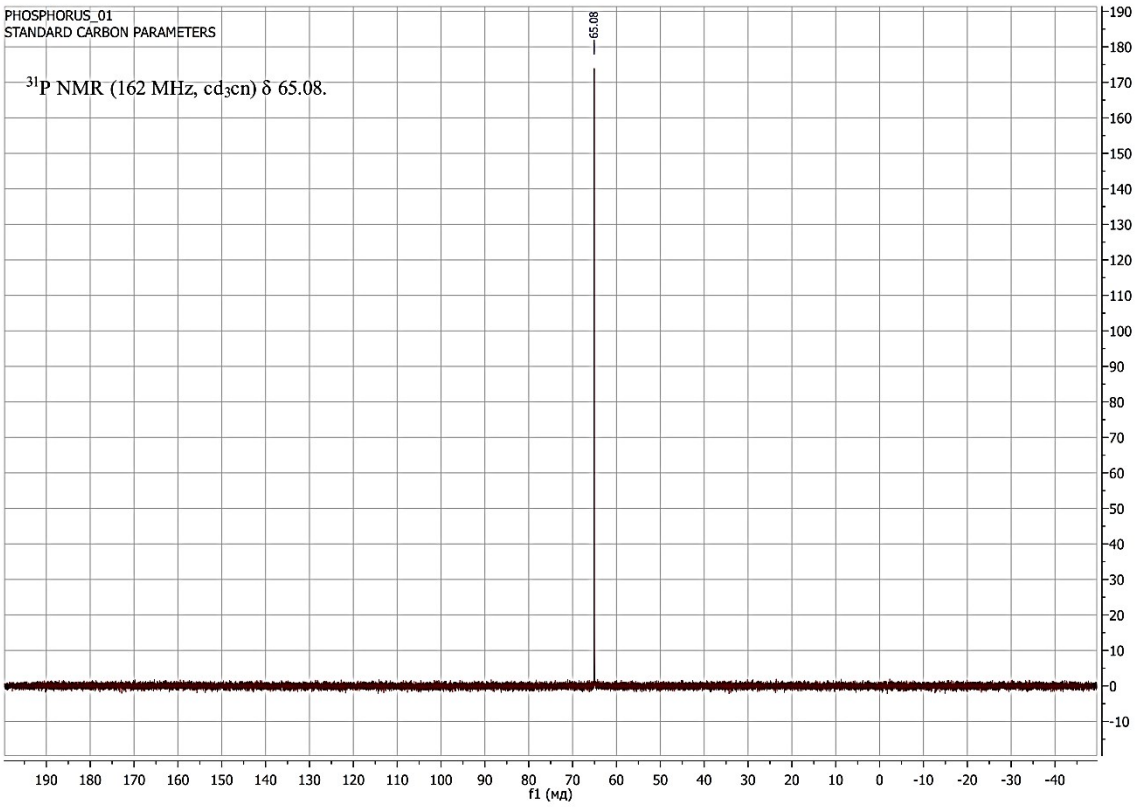

Figure S17. $^{31}P\{^{1}H\}$ NMR for **1**.

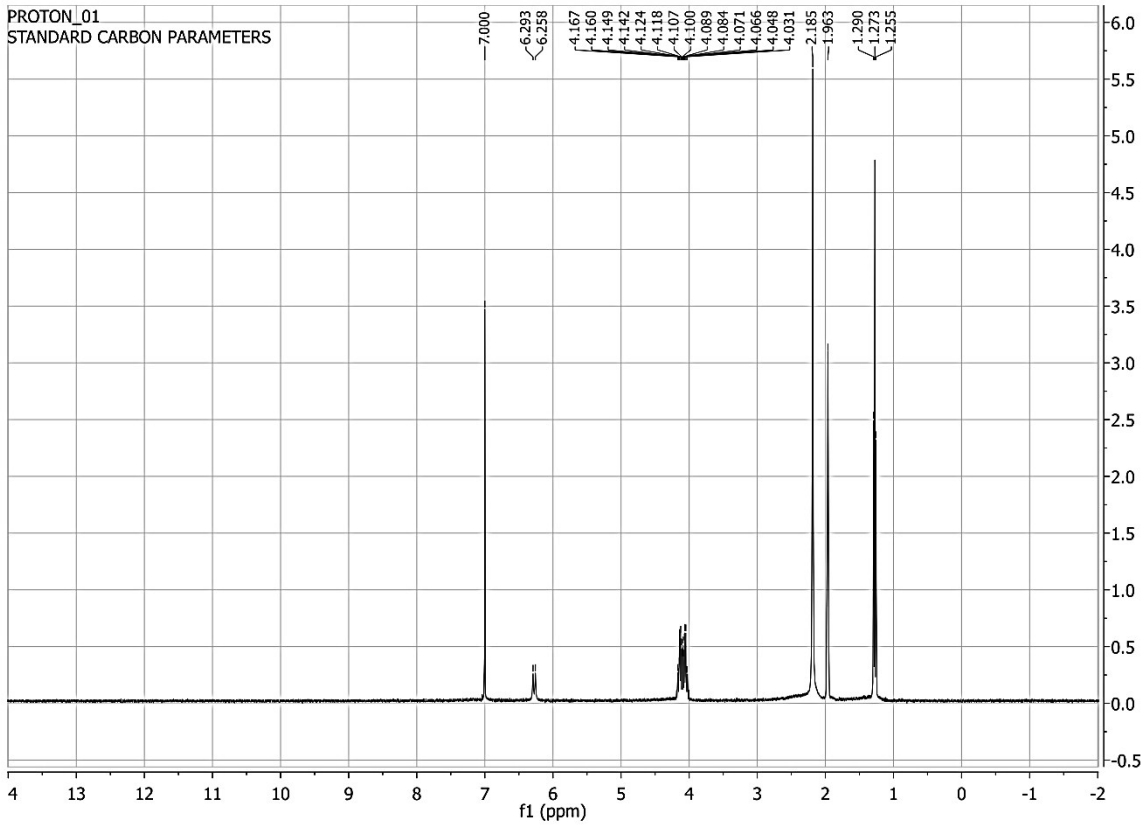

Figure S18. ^{1}H NMR for **1**.

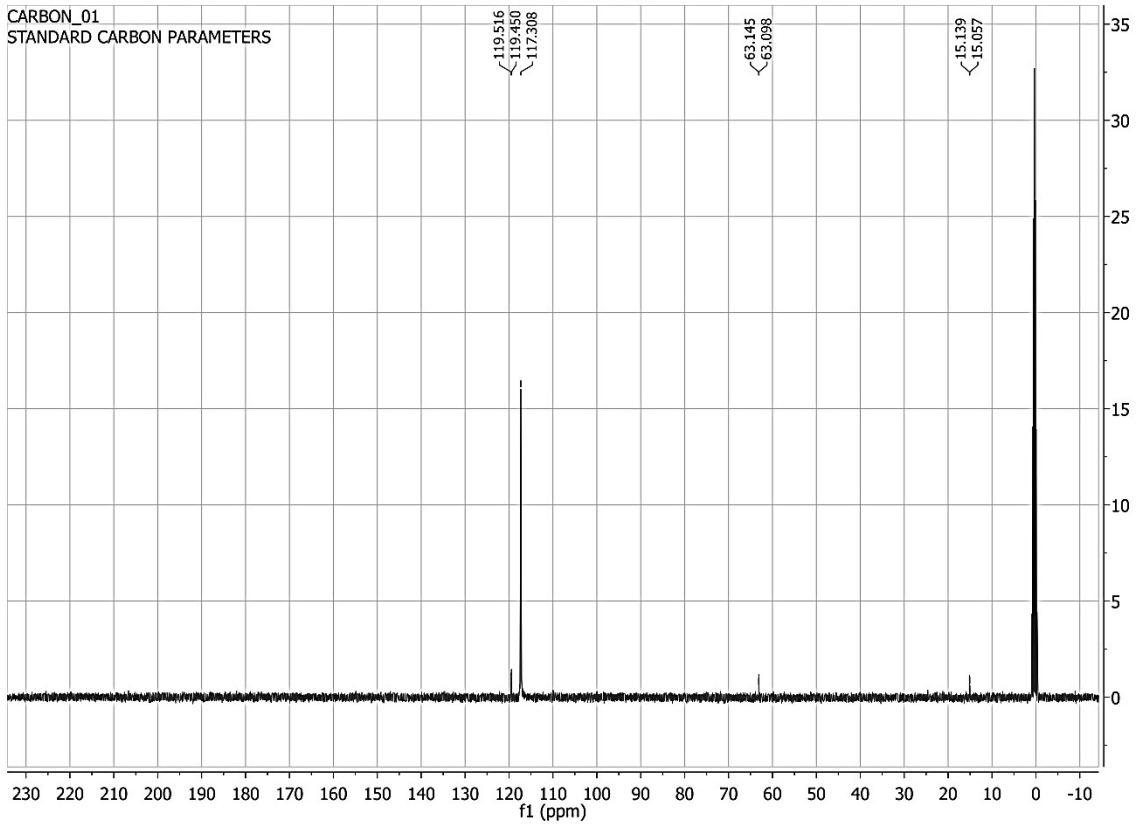

Figure S19. ^{13}C NMR for **1**.

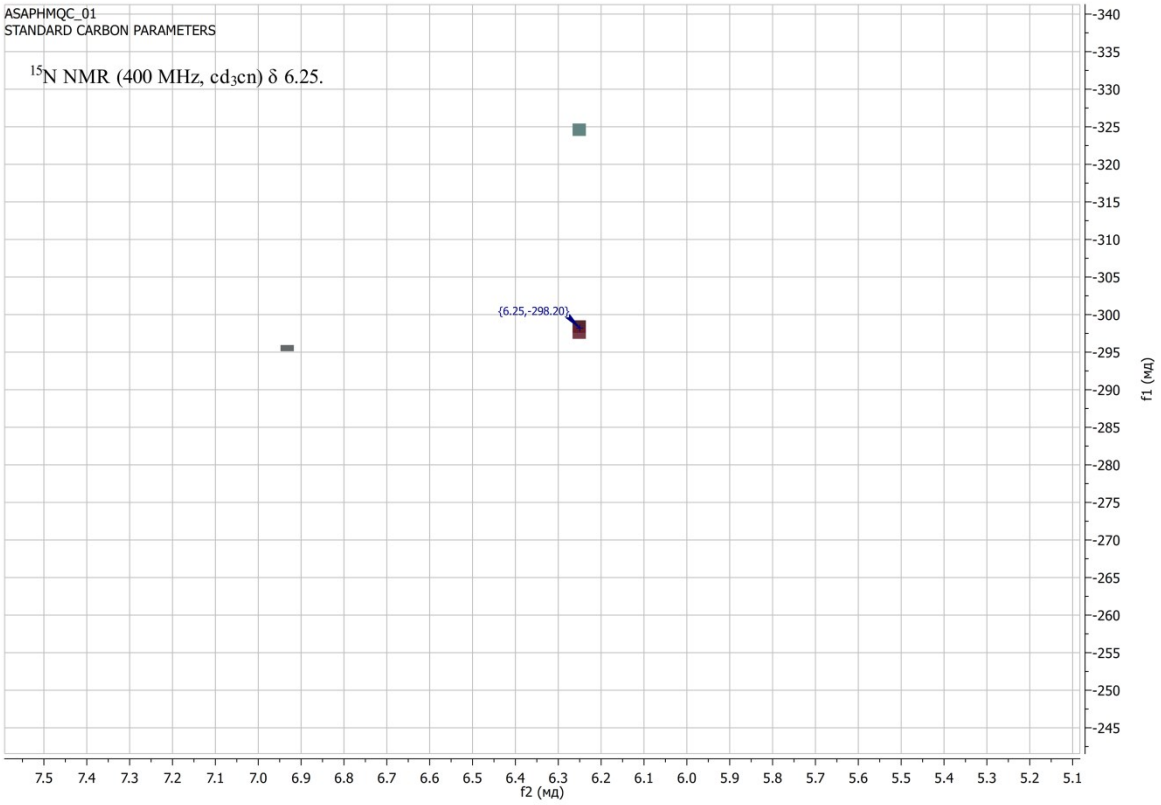

Figure S20. ^{1}H-^{15}N HSQC for **1**.

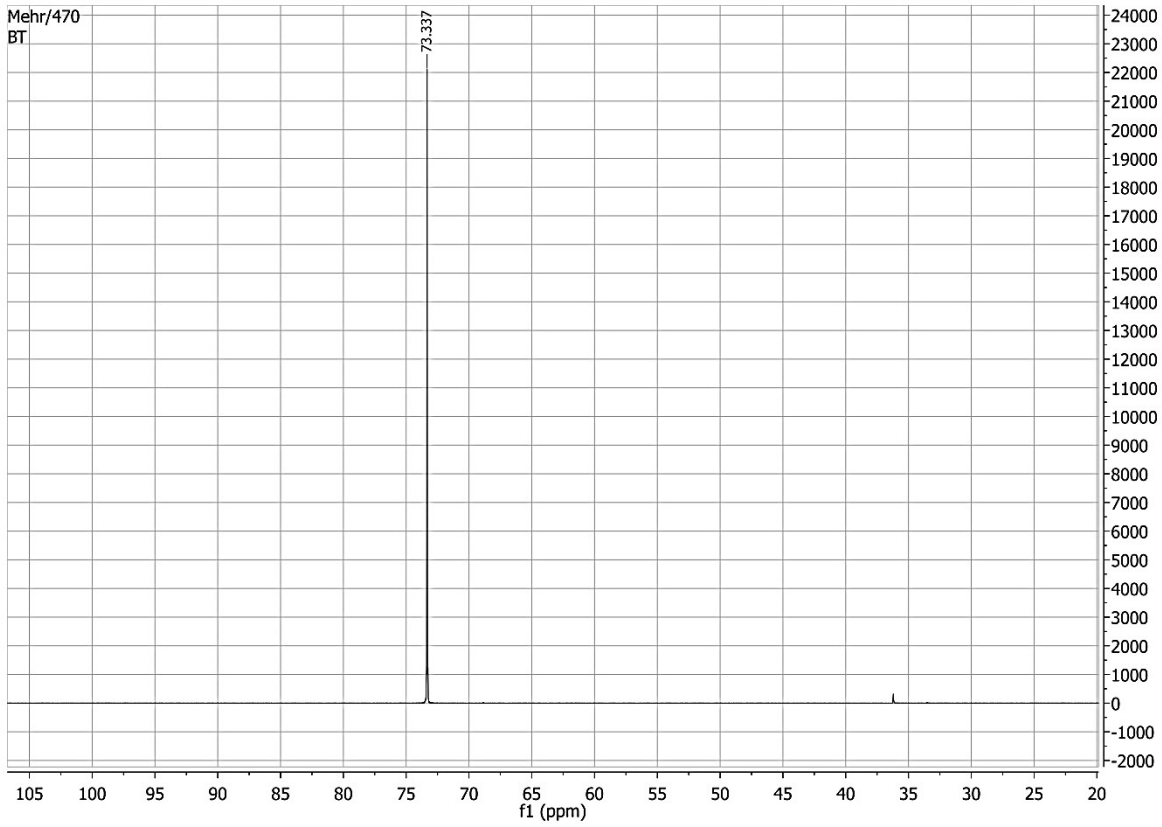

Figure S21. $^{31}P\{^{1}H\}$ NMR for **3**.

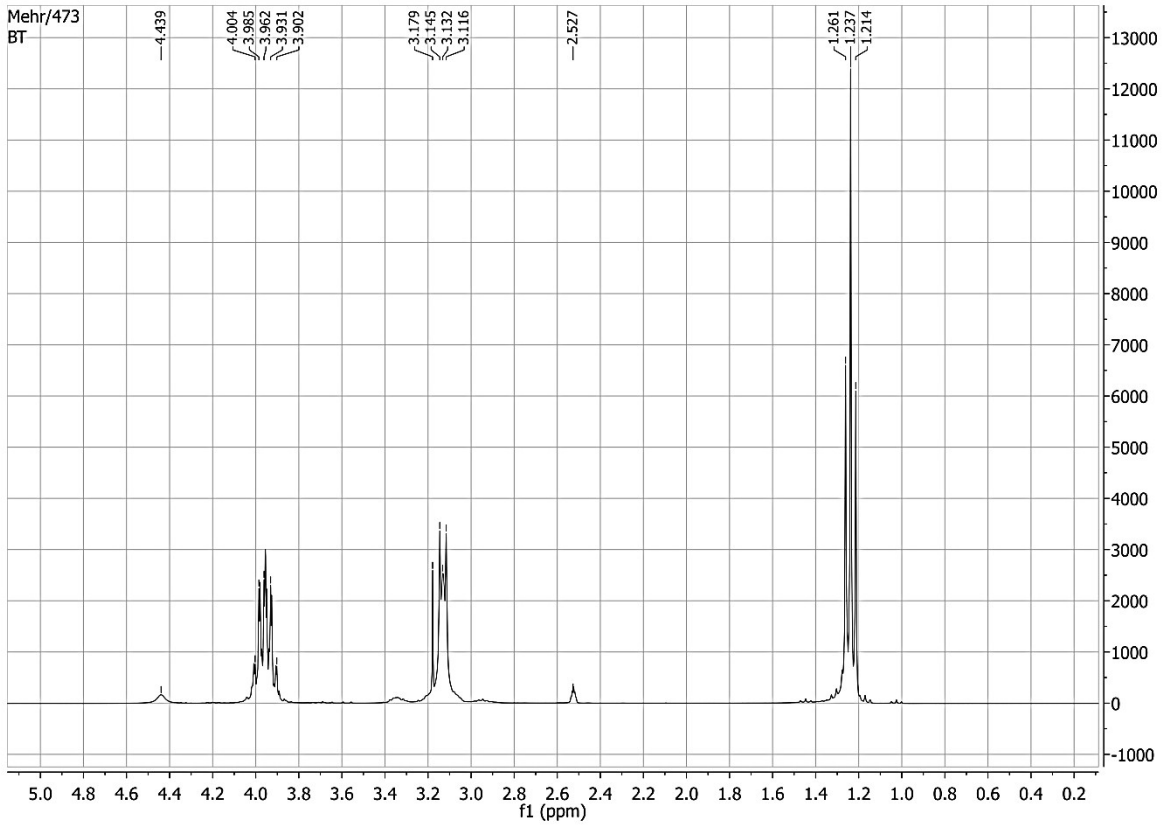

Figure S22. ^{1}H NMR for **3**.

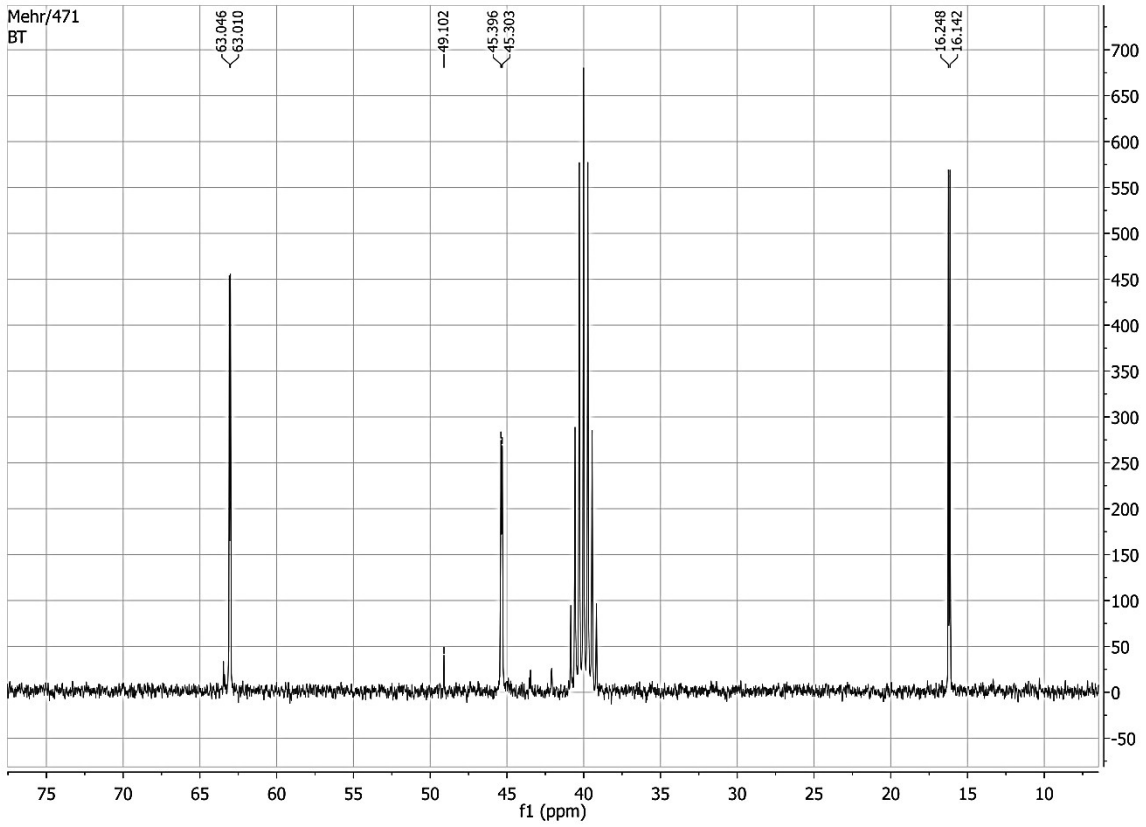

Figure S23. ^{13}C NMR for **3**.

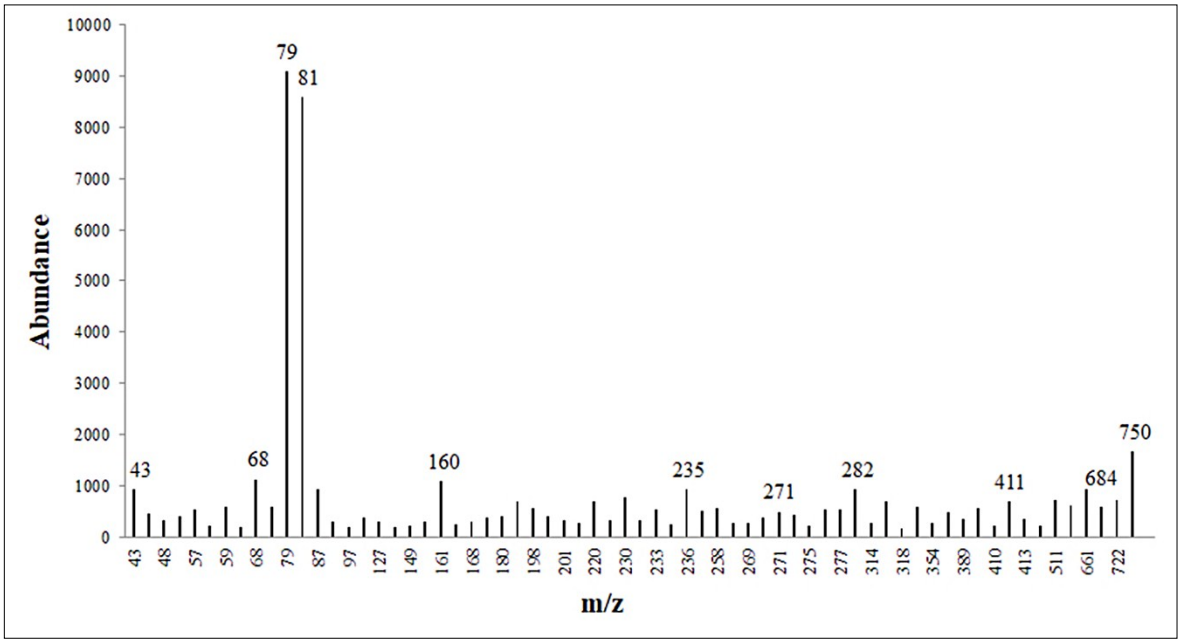

Figure S24. The mass spectrum of **1** at 20 eV experiment.

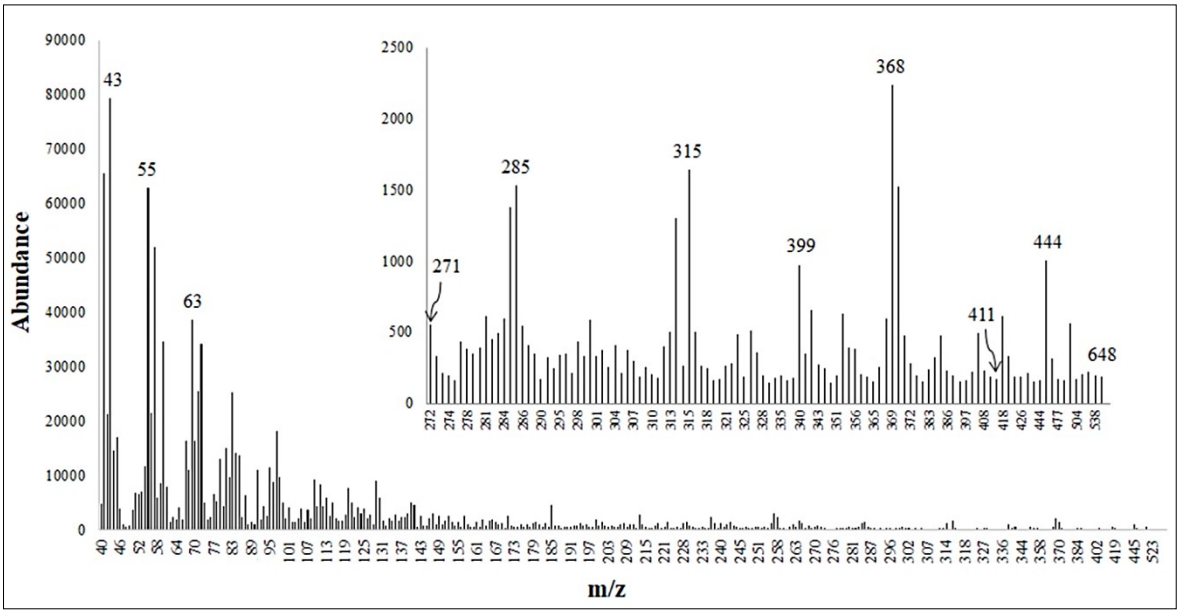

Figure S25. The mass spectrum of **1** at 70 eV experiment.

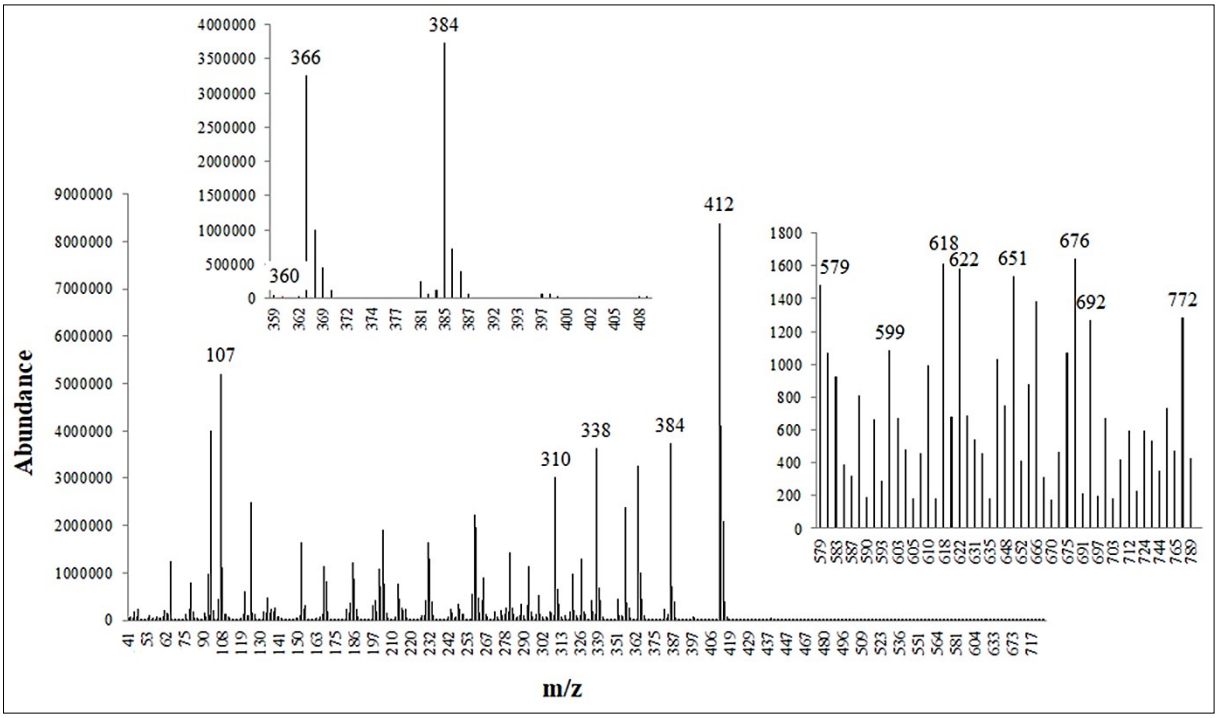

Figure S26. The mass spectrum of **2** at 20 eV experiment.

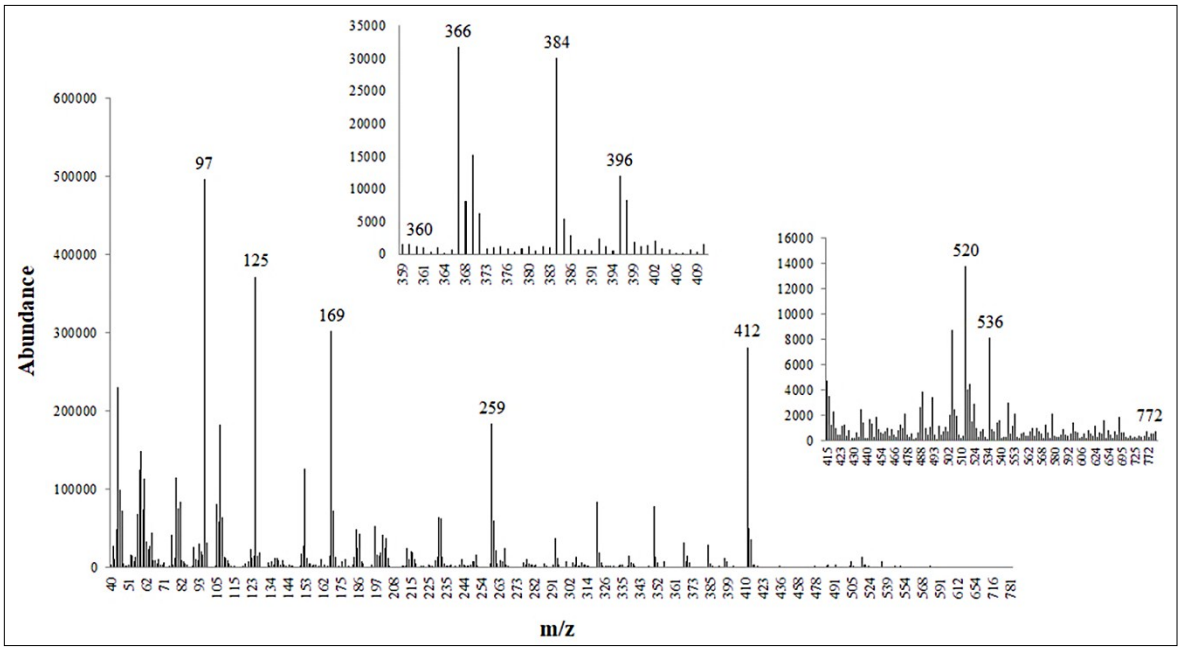

Figure S27. The mass spectrum of **2** at 70 eV experiment.

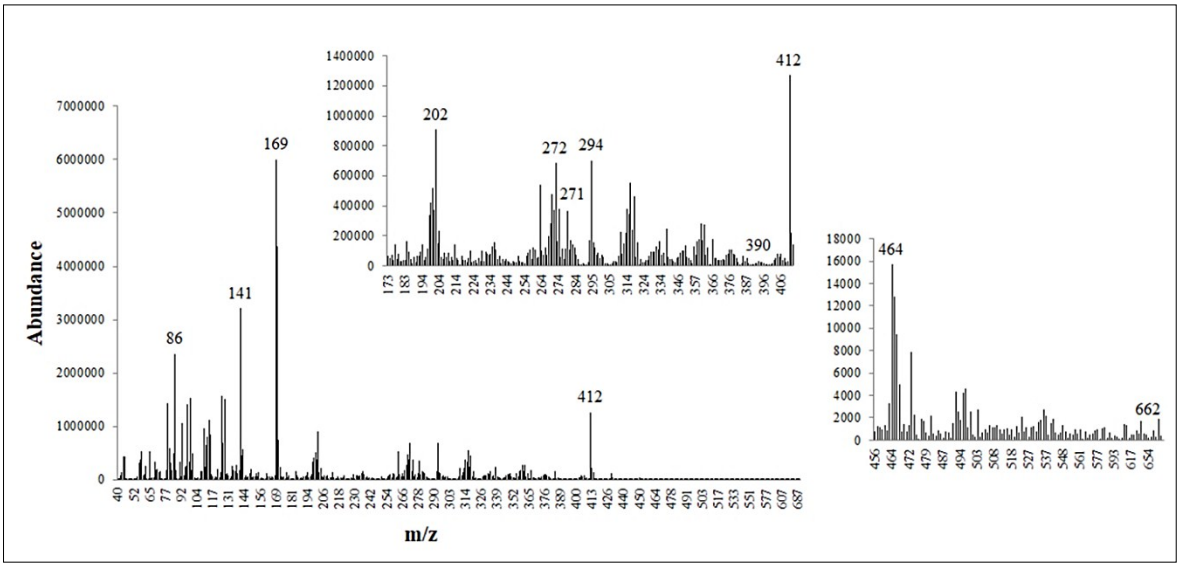

Figure S28. The mass spectrum of **3** at 20 eV experiment.

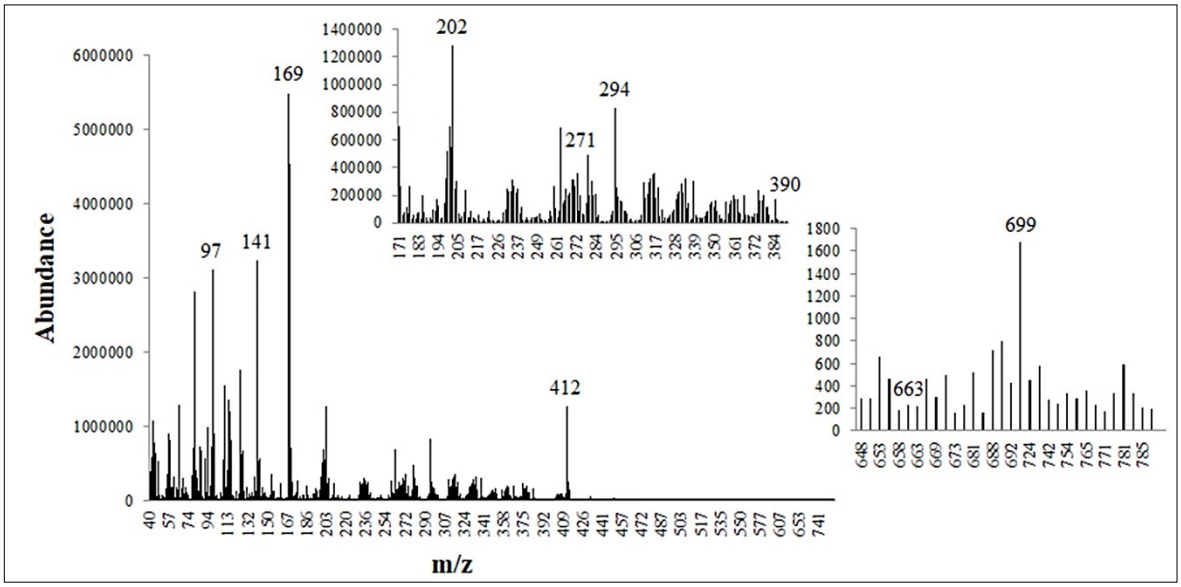

Figure S29. The mass spectrum of **3** at 70 eV experiment.